

Lung epithelial apoptosis in influenza virus pneumonia: the role of macrophage-expressed TNF-related apoptosis-inducing ligand

Susanne Herold,¹ Mirko Steinmueller,¹ Werner von Wulffen,¹ Lidija Cakarova,¹ Ruth Pinto,² Stephan Pleschka,² Matthias Mack,³ William A. Kuziel,⁴ Nadia Corazza,⁵ Thomas Brunner,⁵ Werner Seeger,¹ and Juergen Lohmeyer¹

¹University of Giessen Lung Center, Department of Internal Medicine, Division of Pulmonary and Critical Care Medicine and Infectious Diseases, and ²Institute of Medical Virology, Justus-Liebig-University, 35390 Giessen, Germany

³Klinikum, Department of Internal Medicine, University of Regensburg, D-93042 Regensburg, Germany

⁴PDL BioPharma Inc., Redwood City, CA 94063

⁵Institute of Pathology, Division of Immunopathology, University of Bern, CH 3010 Bern, Switzerland

Mononuclear phagocytes have been attributed a crucial role in the host defense toward influenza virus (IV), but their contribution to influenza-induced lung failure is incompletely understood. We demonstrate for the first time that lung-recruited "exudate" macrophages significantly contribute to alveolar epithelial cell (AEC) apoptosis by the release of tumor necrosis factor-related apoptosis-inducing ligand (TRAIL) in a murine model of influenza-induced pneumonia. Using CC-chemokine receptor 2-deficient (CCR2^{-/-}) mice characterized by defective inflammatory macrophage recruitment, and blocking anti-CCR2 antibodies, we show that exudate macrophage accumulation in the lungs of influenza-infected mice is associated with pronounced AEC apoptosis and increased lung leakage and mortality. Among several proapoptotic mediators analyzed, TRAIL messenger RNA was found to be markedly up-regulated in alveolar exudate macrophages as compared with peripheral blood monocytes. Moreover, among the different alveolar-recruited leukocyte subsets, TRAIL protein was predominantly expressed on macrophages. Finally, abrogation of TRAIL signaling in exudate macrophages resulted in significantly reduced AEC apoptosis, attenuated lung leakage, and increased survival upon IV infection. Collectively, these findings demonstrate a key role for exudate macrophages in the induction of alveolar leakage and mortality in IV pneumonia. Epithelial cell apoptosis induced by TRAIL-expressing macrophages is identified as a major underlying mechanism.

CORRESPONDENCE

Susanne Herold:
Susanne.Herold@
innere.med.uni-giessen.de

Abbreviations used: AEC, alveolar epithelial cell; BAL, bronchoalveolar lavage; BALF, BAL fluid; CCL2, CC-chemokine ligand 2; CCR2, CC-chemokine receptor 2; FasL, Fas ligand; IV, influenza virus; mRNA, messenger RNA; pi, post infection; TRAIL, TNF-related apoptosis-inducing ligand.

Influenza viruses (IVs) may cause primary viral pneumonia in humans with fatal outcome as soon as the pathogen spreads from the upper respiratory tract to the alveolar air space, especially during infections with highly pathogenic IV. Early innate immune responses initiate the release of proinflammatory chemokines and the recruitment of neutrophils, lymphocytes, and particularly mononuclear phagocytes into the alveolar air space to limit viral spread (1). The mononuclear phagocyte system of the lung is composed of resident interstitial and alveolar macrophages (F4/80⁺CD11c^{high}MHCII^{low}) and pulmonary DCs (F4/80⁺CD11c^{high}MHCII^{high}),

both derived from a common BM precursor (2, 3). During lung inflammation and IV infection, peripheral blood monocytes (GR1^{int}F4/80⁺CD11c⁻CD11b⁺CD115⁺) are recruited to the alveolar compartment of the lung via the interaction of CC-chemokine ligand 2 (CCL2), which is released from alveolar epithelial cells (AECs) with its monocytic receptor CC-chemokine receptor 2 (CCR2) (1, 4–6).

© 2008 Herold et al. This article is distributed under the terms of an Attribution–Noncommercial–Share Alike–No Mirror Sites license for the first six months after the publication date (see <http://www.jem.org/misc/terms.shtml>). After six months it is available under a Creative Commons License (Attribution–Noncommercial–Share Alike 3.0 Unported license, as described at <http://creativecommons.org/licenses/by-nc-sa/3.0/>).

These “exudate” macrophages acquire a lung resident macrophage phenotype and finally replenish the alveolar macrophage pool during the time course of infection (7).

Besides their essential host defense functions, mononuclear phagocytes have been proposed to contribute to an imbalanced detrimental immune response during IV pneumonia (8, 9) and have been implicated in alveolar epithelial damage. Human IV pneumonia, which is characterized by rapid progression to lung failure and poor outcome, has gained in importance during the recent outbreaks in Southeast Asia. Infection with highly pathogenic IV causes significant tissue damage to the lungs with acute alveolitis followed by massive pulmonary edema and hemorrhage and extensive destruction of the respiratory epithelium (10–12). However, the distinct molecular steps of macrophage–epithelial interaction during IV-induced acute lung injury remain elusive.

Several authors suggest AEC apoptosis to be an underlying mechanism of alveolar damage in murine and human models of adult respiratory distress syndrome (13–15). Death receptors and their ligands play an important role in the orchestration of innate and adaptive immune responses (16–18). TNF-related apoptosis-inducing ligand (TRAIL) is a transmembrane protein belonging to the TNF superfamily. Among the members of this family, TRAIL exhibits the highest homology to Fas ligand (FasL), a well known inducer of programmed cell death (18). Being expressed mainly on T cells, NK cells, and mononuclear phagocyte subsets, murine TRAIL exerts its proapoptotic signals via binding to DR5 (death receptor 5) (19) and displays potent antitumor activity (20, 21). Recently, an antiviral function in experimental murine IV infection has been suggested (18). However, the contribution of TRAIL to alveolar epithelial apoptosis and lung barrier dysfunction during lethal IV pneumonia has not been elucidated yet.

In the present study, in a murine model of IV-induced acute lung injury, we demonstrate for the first time that exudate macrophages recruited via the CCL2–CCR2 axis largely contribute to AEC apoptosis involving the expression of TRAIL. Both blockade of the specific chemokine–receptor axis and abrogation of macrophage TRAIL signaling by anti-TRAIL mAb treatment or use of adoptively transferred mice recruiting TRAIL-deficient exudate macrophages significantly reduced alveolar epithelial apoptosis and lung leakage in infected mice, resulting in increased survival during otherwise fatal IV pneumonia.

RESULTS

Genetic deletion of CCR2 reduces mortality, morbidity, and alveolar barrier dysfunction during PR/8 infection

Previous reports suggest that the chemokine receptor CCR2 is critically involved in host immune responses to lung infection (4, 22–24). To investigate the influence of CCR2 on the course of IV pneumonia in mice, C57BL/6 WT and CCR2^{-/-} mice were intratracheally inoculated with a lethal dose of the mouse-adapted IV strain PR/8, and survival and body weight were determined during the 21 d post infection (pi).

As shown in Fig. 1 A, only 17.3% of CCR2-deficient mice succumbed to PR/8 infection as compared with 78.4% of infected WT mice ($P < 0.005$ on days 14–21 pi). Likewise, body weight loss was significantly less in CCR2^{-/-} mice on days 8, 9, and 11 pi. To evaluate whether the observed differences in morbidity and mortality during PR/8 infection were associated with increased severity of lung injury in WT mice as compared with CCR2^{-/-} mice, alveolar barrier function was assessed during a time course of 21 d after PR/8 infection in the two treatment groups. Indeed, alveolar leakage was significantly reduced in CCR2-deficient mice on day 7 pi (1.25 ± 0.39 vs. 0.54 ± 0.37 arbitrary units; Fig. 1 B), indicating that CCR2^{-/-} mice develop less alveolar barrier damage upon PR/8 infection than WT mice.

During IV pneumonia, alveolar epithelial injury may be caused by direct cytopathic effects of IV replicating primarily in epithelial cells. Therefore, we evaluated whether the observed differences in lung barrier damage between WT and CCR2^{-/-} mice were linked to different viral replication efficiencies in the lung tissue of the two mouse strains. Analyses of viral replication in lung homogenates from PR/8-infected WT compared with CCR2^{-/-} mice revealed no significant differences in peak viral titers at days 2, 3, and 5 pi and even slightly elevated virus titers in CCR2^{-/-} mice during the later stages of infection ($1.05 \pm 1.33 \times 10^3$ vs. $6.20 \pm 3.90 \times 10^3$ foci-forming units/lung on day 11 pi; Fig. 1 C). These

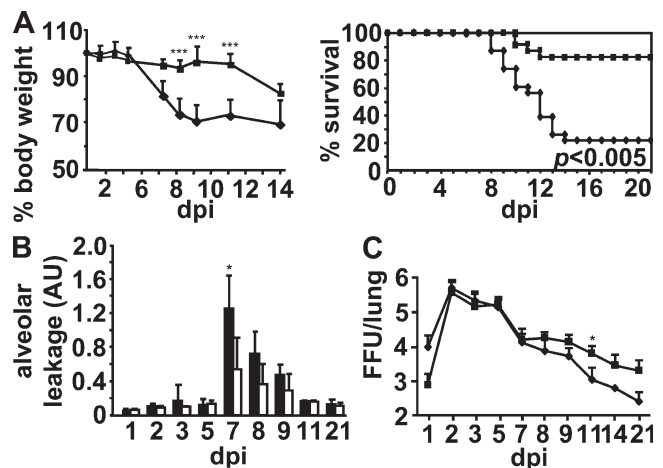


Figure 1. CCR2 deficiency is associated with increased survival, reduced body weight loss, attenuated alveolar leakage, and slightly reduced viral clearance during the time course of PR/8 infection. (A) Body weight and survival of PR/8-infected sex- and age-matched WT (◆, $n = 23$) or CCR2^{-/-} (■, $n = 23$) were determined until days 14 and 21 pi, respectively in four independent experiments. Error bars show SD. (B) Alveolar leakage was analyzed in PR/8-infected WT (filled bars) or CCR2^{-/-} (empty bars) mice. The ratio of BALF and blood FITC fluorescence is expressed in arbitrary units (AU). (C) Lung virus titers of WT (◆) and CCR2^{-/-} (■) mice in the time course of PR/8 infection. Virus titers were determined from lung homogenate supernatants and values are given as log₁₀ foci-forming units (FFU)/lung. Data in B and C are means \pm SD of three to five mice per group from at least three independent experiments. *, $P < 0.05$; ***, $P < 0.005$.

results indicate that enhanced alveolar injury in WT mice during PR/8 pneumonia is not caused by higher viral replication rates than those in *CCR2*^{-/-} mice and rather suggest that mononuclear phagocytes recruited to inflamed tissues in a *CCR2*-dependent manner may directly cause alveolar damage during IV pneumonia.

CCR2 deficiency selectively affects alveolar mononuclear phagocyte recruitment during IV pneumonia

To evaluate whether the amount and composition of alveolar leukocyte infiltration differ in PR/8-infected WT and *CCR2*^{-/-} mice, total bronchoalveolar lavage (BAL) fluid (BALF) cell

counts and cell differentials were determined at various time points pi. No significant differences in total BALF cell counts were detectable between the two treatment groups (Fig. 2 A). Peak alveolar neutrophil accumulation was delayed in *CCR2*-deficient mice and slightly exceeded values reached in WT mice on days 7 and 8 pi. Lymphocyte recruitment was virtually identical in both treatment groups. Total numbers of resident alveolar macrophages in BALF were lower in *CCR2*-deficient mice on days 5–9 pi but reached comparable levels during the later stages of infection. However, alveolar mononuclear phagocyte recruitment was found to be strongly reduced in *CCR2*-deficient mice, most prominently at day 8

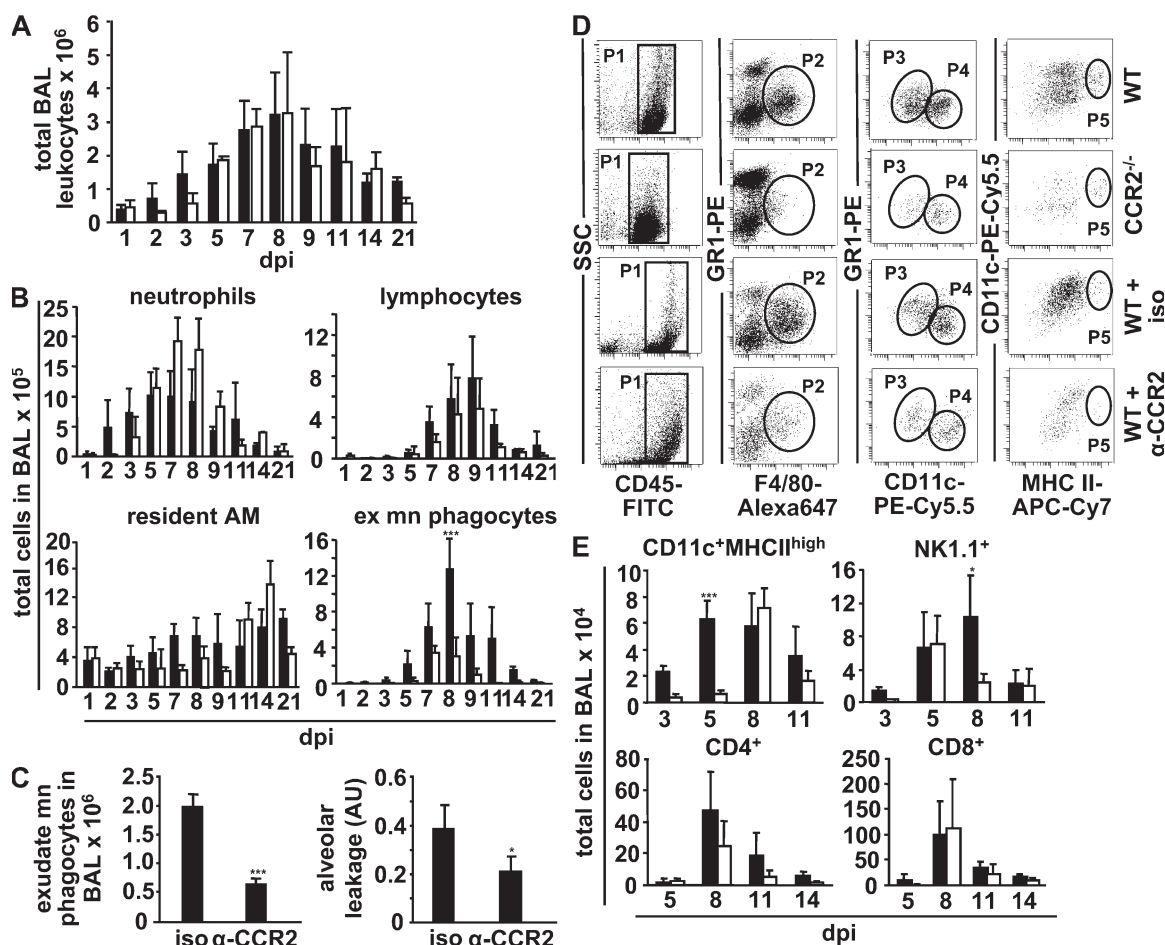


Figure 2. Alveolar macrophage recruitment in PR/8-infected mice is *CCR2* dependent. (A and B) PR/8-infected WT (filled bars) or *CCR2*^{-/-} (empty bars) mice were subjected to BAL, followed by quantification of total leukocyte BALF numbers (A) and BAL leukocyte subpopulations (B) from Pappenheim-stained cytocentrifuge preparations. (C) Quantification of exudate mononuclear phagocytes calculated from differential counts of BAL leukocytes from infected WT mice treated with isotype IgG or anti-*CCR2* mAb (day 8 pi, left). Alveolar leakage of isotype- or anti-*CCR2*-treated PR/8-infected mice (day 7 pi, right). (D) FACS analysis of alveolar mononuclear phagocyte subpopulations in BALF from infected WT versus *CCR2*^{-/-} mice or from WT mice treated with isotype IgG or anti-*CCR2* mAb was performed by three-hierarchy gating on day 8 pi. CD45⁺ cells (population 1 [P1]) were gated according to their GR1 and F4/80 expression. GR1^{int}F4/80⁺ cells represent alveolar mononuclear phagocytes (population 2 [P2]). Subgate analysis of population 2 revealed a CD11c^{int} (population 3 [P3], exudate macrophages) and a CD11c^{high} (population 4 [P4], resident AM) subpopulation as well as a CD11c^{high}-MHCII^{high} subpopulation (population 5 [P5]) representing alveolar DCs. (E) Flow cytometric quantification of CD11c^{high}MHCII^{high} DCs and lymphocyte subpopulations from BAL leukocytes of PR/8-infected WT (filled bars) versus *CCR2*^{-/-} (empty bars) mice using the gating characteristics described in D for DCs. For analysis of lymphocyte subpopulations, CD45⁺ cells were subgated on NK cells (SSC^{low}NK1.1⁺), CD4 T cells (SSC^{low}CD4⁺), and CD8 T cells (SSC^{low}CD8⁺). Data in E are given as total cells in BAL calculated from the respective percentage of CD45⁺ cells. All bar graphs represent the means ± SD from five experiments. *, P < 0.05; ***, P < 0.005. AM, alveolar macrophages; ex, exudate; mn, mononuclear; iso, isotype IgG.

pi ($1.27 \pm 0.35 \times 10^6$ vs. $0.3 \pm 0.21 \times 10^6$; Fig. 2 B). Correspondingly, exudate mononuclear phagocyte numbers were significantly decreased in PR/8-infected WT mice pretreated with an anti-CCR2 mAb by day 8 pi (Fig. 2 C, left), which is associated with reduced alveolar leakage, as compared with isotype IgG-treated mice (Fig. 2 C, right), suggesting a key role of alveolar recruited mononuclear phagocytes in IV-induced lung barrier breakdown.

To further dissect the alveolar mononuclear phagocyte subset composition, BALF cells gained from PR/8-infected mice of the various treatment groups were subjected to FACS analysis for surface marker expression at day 8 pi. Analysis of CD45⁺ BALF cells (population 1; Fig. 2 D, first column) for

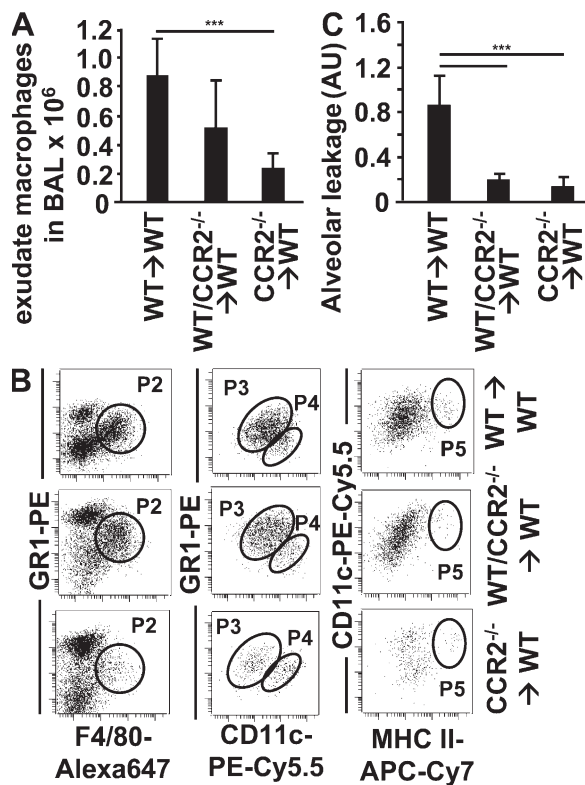


Figure 3. Alveolar barrier dysfunction is associated with CCR2 expression on circulating leukocytes during PR/8 infection. (A) Three different groups of PR/8-infected BM chimeric mice (WT recipient mice with transplantation of 100% WT BM cells; WT recipient mice with transplantation of mixed 50% WT/ 50% CCR2^{-/-} BM cells; and WT recipient mice with transplantation of 100% CCR2^{-/-} BM cells) were subjected to BAL at day 8 pi. Exudate macrophage numbers were calculated from BAL leukocyte numbers and differential counts of Papanheim-stained cyto-centrifuge preparations. (B) FACS analysis of BALF cells from PR/8-infected chimeric mice of each transplantation group was performed as described in Fig. 2 D, and representative dot plots from three independent experiments are shown. Note that population 3 (P3; exudate macrophages), population 4 (P4; resident alveolar macrophages), and population 5 (P5; alveolar DCs) are subgates of population 2 [P2]. (C) Alveolar leakage from PR/8-infected chimeric mice at day 7 pi. All bar graphs represent the means \pm SD of four to eight mice per group from three independent experiments. ***, $P < 0.005$.

GR1 and F4/80 expression revealed three distinct cell populations: GR1^{high}F4/80⁻ neutrophils, GR1⁻F4/80⁻ lymphocytes, and GR1^{int}F4/80⁺ mononuclear phagocytes (population 2; Fig. 2 D, second column), which were composed of a CD11c^{int} (population 3, henceforth termed exudate macrophages) and

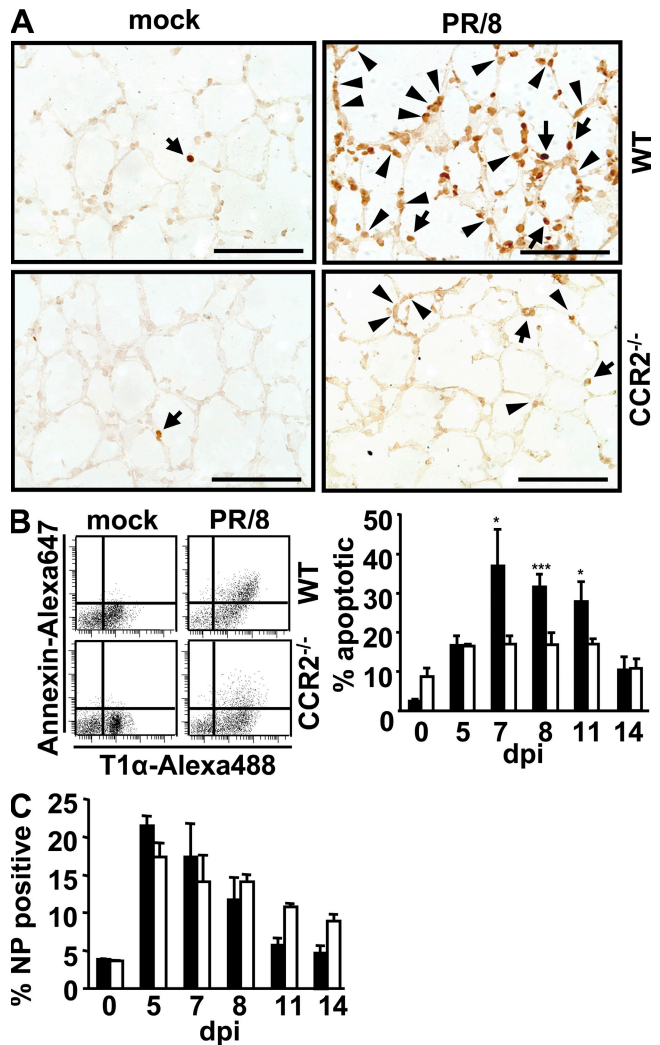


Figure 4. AEC apoptosis is reduced in PR/8-infected CCR2^{-/-} mice compared with WT mice. (A) WT or CCR2^{-/-} mice were mock or PR/8 infected and TUNEL assay was performed on cryosections from lavaged lungs at day 7 pi. Nuclei of apoptotic cells appear in brown. Arrows, apoptotic intraalveolar leukocytes; arrowheads, apoptotic AEC. Bars, 100 μ m. (B) Flow cytometric quantification of apoptotic AEC. Lungs from mock- or PR/8-infected WT or CCR2^{-/-} mice were digested on day 7 pi and analyzed for annexin V binding. Representative dot plots show expression of the AEC type I marker T1 α and annexin V staining of viable (propidium iodide negative) CD45⁻ cells. Apoptotic cells are mainly AEC type I (left). Quantification of FACS data as obtained in B from PR/8-infected mice (right). The bar graph represents the annexin V⁺ proportion of CD45⁻ T1 α ⁺ cells. (C) Quantification of FACS analysis of the NP⁺ proportion of CD45⁻ T1 α ⁺ cells from lung homogenates in the time course after PR/8 infection. Values are means \pm SD of three to four mice per group from three independent experiments. *, $P < 0.05$; ***, $P < 0.005$. NP, IV nucleoprotein; filled bars, WT; empty bars, CCR2^{-/-}.

a CD11c^{high} (population 4) subpopulation, representing resident alveolar macrophages according to previous reports (2, 3). Exudate macrophages (population 3) accumulated to a much lesser extent in CCR2^{-/-} mice or in mice pretreated with anti-CCR2 antibody as compared with WT mice or isotype IgG-treated mice, respectively (Fig. 2 D, third column). Alveolar mononuclear phagocytes (population 2) contained a low proportion of DCs (CD11c⁺MHCII^{high} [population 5 (P5)]; Fig. 2 D, fourth column). Alveolar DC recruitment was delayed in PR/8-infected CCR2^{-/-} mice but reached peak values comparable to those of WT mice by day 8 pi (Fig. 2 E, top left). Flow cytometric analysis of alveolar lymphocyte subsets revealed no striking differences in the recruitment of CD4⁺ T cells or CD8⁺ T cells between WT and CCR2-deficient mice at the given time points, whereas alveolar NK cell accumulation peaked earlier at day 5 pi in CCR2^{-/-} mice (Fig. 2 E). Analysis of interstitial exudate macrophage accumulation in PR/8-infected lungs revealed faster recruitment kinetics than in the alveolar compartment but was likewise significantly reduced in mice lacking CCR2 (Fig. S1, available at <http://www.jem.org/cgi/content/full/jem.20080201/DC1>). Altogether, our data demonstrate that recruitment of GR1^{int}F4/80⁺CD11c^{int}MHCII^{low} exudate macrophages into the lungs during PR/8 pneumonia was severely impaired in CCR2-deficient mice or WT animals treated with function blocking anti-CCR2 antibodies.

CCR2 expression on circulating leukocytes, but not on lung resident cells, is associated with alveolar barrier dysfunction during PR/8 infection

To distinguish whether CCR2 expressed on resident lung cells, such as resident alveolar macrophages or AEC, or CCR2 present on circulating leukocytes accounted for the increased IV-induced alveolar leakage in WT versus CCR2^{-/-} mice, we made use of a BM chimeric mouse model. We established three different transplantation groups: (a) WT mice with transplantation of 100% WT BM cells; (b) WT mice with transplantation of a mixture of WT and CCR2^{-/-} BM cells (50% WT/50% CCR2^{-/-}); and (c) WT mice with transplantation of 100% CCR2^{-/-} BM cells. CCR2 expression on F4/80⁺ peripheral blood monocytes was analyzed 14 d after transplantation by flow cytometry and corresponded to the respective proportion of transplanted WT or CCR2^{-/-} BM cells in the different transplantation groups, whereas resident alveolar macrophages homogeneously displayed a WT phenotype as previously outlined in detail (25) (unpublished data). Exudate macrophage accumulation on day 8 after PR/8 infection in transplanted mice was dependent on the proportion of peripheral blood monocytes with intact CCR2 expression, with mice after transplantation of WT BM recruiting $0.85 \pm 0.27 \times 10^6$, mice after transplantation of mixed BM recruiting $0.57 \pm 0.29 \times 10^6$, and mice after transplantation of CCR2^{-/-} BM recruiting a total of $0.24 \pm 0.09 \times 10^6$ exudate macrophages into the alveolar compartment (Fig. 3, A and B). Notably, alveolar leakage at day 7 pi was significantly reduced in mice after transplantation of CCR2^{-/-} BM com-

pared with mice after transplantation of 100% WT BM (Fig. 3 C). These results clearly demonstrate that CCR2 expressed on circulating blood monocytes is critically involved in mononuclear phagocyte extravasation into the alveolar compartment of the lung, thereby contributing to alveolar barrier dysfunction during IV pneumonia.

CCR2-dependent alveolar exudate macrophage accumulation is associated with increased AEC apoptosis

Given that the CCR2-dependent accumulation of exudate macrophages in IV pneumonia contributed to the loss of alveolar barrier integrity, we hypothesized that this recruited mononuclear cell population might promote barrier dysfunction by inducing AEC apoptosis. Therefore, cryosections from lavaged lungs of mock- or PR/8-infected WT or CCR2-deficient mice were subjected to TUNEL assay. As shown in Fig. 4 A, the number of apoptotic alveolar cells was strikingly less in PR/8-infected CCR2^{-/-} mice as compared with WT mice, and virtually undetectable in mock-infected

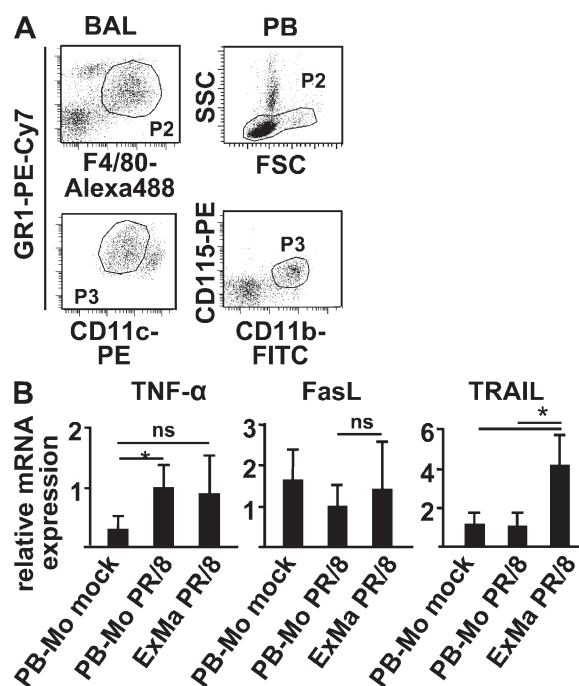


Figure 5. Relative mRNA expression of the proapoptotic factors TNF- α , TRAIL, and FasL in peripheral blood (PB) monocytes and alveolar exudate macrophages. (A) BALF exudate alveolar macrophages from PR/8-infected WT mice were high-purity flow sorted on day 8 pi according to their surface expression of F4/80, GR1, and CD11c (F4/80⁺GR1^{int}CD11c^{int} [population 3 (P3)], left). PB monocytes from the same (PR/8 infected) animals or from mock-infected mice were flow sorted according to their scatter characteristics (SSC^{low}) and CD11b and CD115 expression (CD11b⁺CD115⁺ [population 3 (P3)], right). SSC, side scatter; FSC, forward scatter. (B) Relative mRNA expression of TNF- α , TRAIL, and FasL from sorted PB monocytes of mock-infected (PB-Mo mock) or PR/8-infected (PB-Mo PR/8) mice or from exudate macrophages of infected mice (ExMa PR/8). Values are the means \pm SD from three independent experiments, including pooled BALF or blood cells, from $n = 8$ mice each. *, $P < 0.05$.

mice. For apoptosis quantification of AEC type I representing the major component of the alveolar surface, lung homogenates of the respective treatment groups were subjected to flow cytometry, and CD45⁺ cells were analyzed for annexin V binding and expression of the AEC type I marker T1 α . Representative dot plots in Fig. 4 B (left) demonstrate a significantly larger proportion of type I AEC to undergo apoptosis in lung homogenates of PR/8-infected WT mice than in PR/8-infected CCR2-deficient mice at day 7 pi. Flow cytometric quantification during the time course of infection revealed a sustained increase of type I AEC apoptosis in WT compared with CCR2^{-/-} mice throughout days 7–11 pi corresponding to the kinetics of alveolar exudate macrophage accumulation (Fig. 4 B, right). The proportions of infected (IV nucleoprotein⁺) type I AEC were virtually identical in both WT and CCR2-deficient mice, with direct viral cytopathic effects most likely accounting for the observed type I AEC apoptosis rate that was still present in CCR2^{-/-} mice (Fig. 4, B and C). No differences in CD45⁺CD31⁺ lung endothelial cell apoptosis could be detected during days 5–14 in PR/8-infected WT compared with CCR2^{-/-} mice (unpublished data).

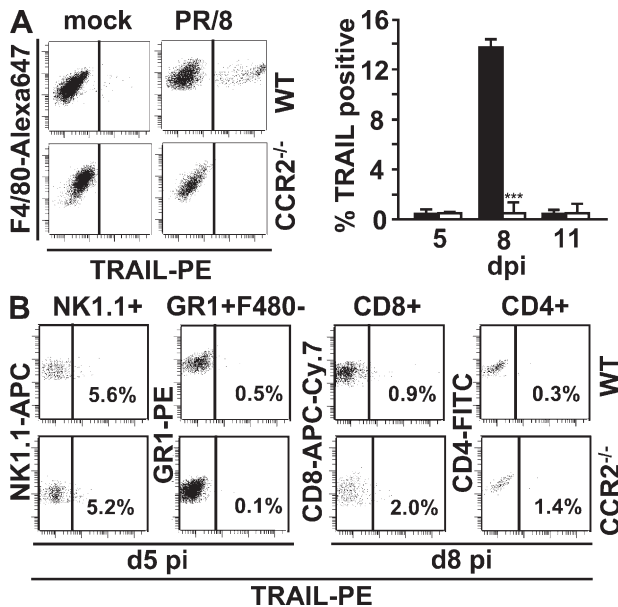


Figure 6. TRAIL is expressed on the cell surface of alveolar exudate macrophages. (A) WT or CCR2^{-/-} mice were mock or PR/8 infected and BAL cells were stained with GR1-FITC, F4/80-Alexa Fluor 647, and TRAIL PE or isotype PE mAbs, respectively. GR1^{int}F4/80⁺ cells were gated and analyzed for TRAIL surface expression (left). Quantitative analysis of the proportion of TRAIL⁺ from F4/80⁺ BALF cells gained from PR/8-infected WT (filled bars) or CCR2^{-/-} mice (empty bars) on days 5, 8, and 11 pi (right). (B) FACS analysis of TRAIL expression on BALF NK cells (SSC^{low}NK1.1⁺), neutrophils (GR1^{high}F4/80⁺), CD8 T cells (SSC^{low}CD8⁺), and CD4 T cells (SSC^{low}CD4⁺) of PR/8-infected WT (top) or CCR2^{-/-} (bottom) mice gained at the indicated time points. Values are the means \pm SD of two to four mice per group from at least two independent experiments. ***, P < 0.005.

Alveolar exudate macrophages up-regulate messenger RNA (mRNA) levels of proapoptotic TRAIL as compared with peripheral blood monocytes

To analyze mRNA levels of potential proapoptotic factors in alveolar exudate macrophages and their blood precursors, peripheral blood monocytes from mock-infected or PR/8-infected WT mice, as well as alveolar exudate macrophages from PR/8-infected WT mice, were flow sorted on day 8 pi according to scatter and surface marker characteristics as shown in Fig. 5 A and analyzed for TNF- α , TRAIL, and FasL transcripts using quantitative RT-PCR. TNF- α mRNA transcripts were found to be significantly increased to the same level in both peripheral blood monocytes and alveolar exudate macrophages from PR/8-infected mice as compared with blood monocytes from mock infected mice (Fig. 5 B, left). However, TNF- α protein levels in BALF did not significantly differ between PR/8-infected WT and CCR2-deficient mice on day 7 pi (348 \pm 65 and 266 \pm 113pg/ml,

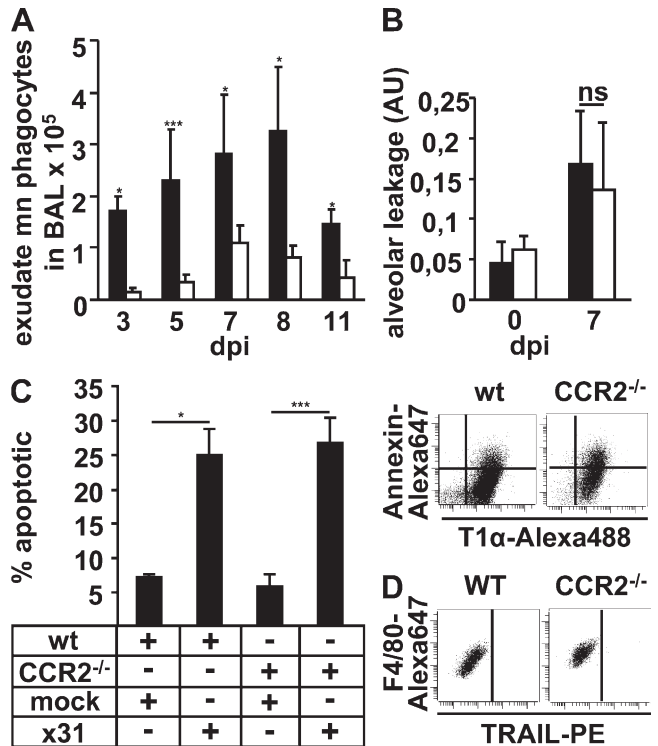


Figure 7. x31-infected WT and CCR2^{-/-} mice lack TRAIL expression on exudate macrophages and reveal equal levels of AEC apoptosis and alveolar barrier function. (A) Quantification of BAL exudate mononuclear phagocytes from Pappenheim-stained cytocentrifuge preparations in x31-infected WT (filled bars) or CCR2^{-/-} (empty bars) mice. (B) Alveolar leakage of uninfected (day 0) or x31-infected (day 7) WT (filled bars) or CCR2^{-/-} (empty bars) mice. (C, right) FACS analysis of apoptotic AEC type I from mock- or x31-infected WT or CCR2^{-/-} mice on day 7 pi. (C, left) Quantification of FACS data. Bar graphs show the annexin V⁺ proportion of CD45⁺ T1 α ⁺ cells. (D) GR1^{int}F4/80⁺ BAL cells from x31-infected WT or CCR2^{-/-} mice were gated and analyzed for TRAIL surface expression. *, P < 0.05; ***, P < 0.005. All bar graphs represent the means \pm SD from three independent experiments.

respectively; unpublished data), suggesting that exudate macrophages recruited to the alveolar space in WT but less in CCR2^{-/-} mice were not the primary source of TNF- α . No significant up-regulation of FasL mRNA could be detected in the analyzed cell populations (Fig. 5 B, middle). In contrast, TRAIL mRNA was selectively up-regulated fourfold in exudate macrophages as compared with their peripheral blood precursors from either mock- or PR/8-infected mice (Fig. 5 B, right).

TRAIL expression in the alveolar space is largely restricted to alveolar exudate macrophages during PR/8 infection

To evaluate TRAIL protein expression on the surface of alveolar mononuclear phagocytes, BALF cells from mock- or PR/8-infected WT or CCR2^{-/-} mice were analyzed by flow cytometry for F4/80 and TRAIL coexpression by day 8 pi. TRAIL was exclusively found on F4/80⁺ BALF cells from PR/8-infected WT but not CCR2-deficient mice, indicating that only CCR2 dependently recruited exudate macrophages but not resident alveolar macrophages expressed TRAIL (Fig. 6 A, left). The proportion of TRAIL⁺ alveolar mononuclear phagocytes (F4/80⁺) raised to \sim 14% in PR/8-infected WT mice on day 8 pi and was always $<$ 1.5% in CCR2-deficient mice in the time course of infection (Fig. 6 A, right). As opposed to previous reports (18), in our model, TRAIL was only expressed on a small proportion of alveolar NK cells (WT, 5.6%; CCR2^{-/-}, 5.2%) and was absent on alveolar CD4⁺ and CD8⁺ T cells as well as on alveolar neutrophils from both WT and CCR2^{-/-} mice at the indicated time points (Fig. 6 B). In addition, TRAIL was undetectable on each of these leukocyte populations including monocytes in peripheral blood (unpublished data).

Absence of TRAIL on alveolar exudate macrophages in x31-infected mice is associated with preservation of alveolar barrier function

Given that PR/8 is highly virulent in mice, we questioned whether exudate macrophages would also act pro-apoptotically toward AECs upon a less severe viral lung infection. Therefore, we infected WT and CCR2-deficient mice with a less pathogenic IV strain, x31, at a nonlethal dose. Upon x31 infection, exudate macrophages accumulated in the alveolar air spaces of WT mice (yet to a lower extent than upon PR/8 infection) and were significantly reduced in the BALF of CCR2^{-/-} mice (Fig. 7 A). However, in contrast to PR/8 infection, x31 induced only a mild alveolar leakage on day 7 pi without differences between WT and CCR2-deficient mice (Fig. 7 B). Accordingly, AEC type I apoptosis was present on day 7 pi (\sim 25%) but no differences were detectable between the two mouse strains (Fig. 7 C). Interestingly, this was correlated to the absence of TRAIL expression on F4/80⁺ alveolar mononuclear phagocytes in x31-infected WT mice (Fig. 7 D), indicating that the induction of TRAIL on exudate macrophages is linked to more severe alveolar inflammation as observed in PR/8 infection.

Anti-TRAIL treatment attenuates alveolar epithelial apoptosis, as well as lung leakage, and enhances survival after PR/8 infection

To evaluate the contribution of exudate macrophage TRAIL to alveolar epithelial apoptosis, TUNEL assay was performed on cryosections of lavaged lungs from PR/8-infected WT mice treated with isotype IgG or anti-TRAIL mAb. Alveolar exudate macrophage numbers in anti-TRAIL- or IgG-treated mice were comparable to those of untreated mice upon PR/8 infection (IgG, $1.97 \pm 0.25 \times 10^6$; anti-TRAIL, $1.83 \pm 0.77 \times 10^6$). As shown in Fig. 8 A, alveolar cell apoptosis was pronounced in isotype IgG-treated mice but significantly decreased in anti-TRAIL-treated mice on day 7 after PR/8 infection. In addition, anti-TRAIL treatment significantly reduced annexin V binding of AEC type I in PR/8-infected lung homogenates as compared with isotype IgG-treated controls (Fig. 8 B). Analysis of alveolar barrier function in anti-TRAIL-treated PR/8-infected WT mice revealed a significant decrease in alveolar leakage in comparison to isotype IgG-treated control mice on day 7 pi (Fig. 8 C). Reduction of alveolar leakage in anti-TRAIL-treated mice was associated with significantly increased survival of IV infection as compared with isotype-treated controls (Fig. 8 D), although viral clearance from PR/8-infected lungs was substantially delayed upon anti-TRAIL treatment in comparison to untreated WT mice (Fig. S2, available at <http://www.jem.org/cgi/content/full/jem.20080201/DC1>). These data clearly demonstrate a crucial role of TRAIL expressed by alveolar exudate macrophages, as opposed to direct viral cytopathic effects, in the development of alveolar barrier dysfunction as a major determinant of mortality during IV pneumonia in mice.

Interestingly, TRAIL receptor (DR5) mRNA transcripts were found to be present in cultured primary murine AEC and were up-regulated upon PR/8 infection in a dose-dependent manner in vitro (Fig. 8 E). Moreover, DR5 was present on type I AEC and further up-regulated on the infected (NP⁺) proportion on day 5 pi in vivo (Fig. 8 F, left). Increased DR5 expression persisted on NP⁺ compared with NP⁻ type I AEC until NP detection was lost by day 14 pi (Fig. 8 F, right), suggesting an enhancing effect of viral infection for macrophage TRAIL-mediated alveolar injury.

AEC apoptosis and leakage are attenuated in PR/8-infected mice recruiting TRAIL-deficient exudate macrophages to the alveolar air space

To strengthen the hypothesis that alveolar exudate macrophage accumulation mediates TRAIL-induced injury in PR/8 pneumonia, the following BM chimeric mice were PR/8 infected 2 wk after transplantation and analyzed for epithelial apoptosis and barrier dysfunction: (a) WT mice with transplantation of WT BM; (b) WT mice with transplantation of TRAIL^{-/-} BM; and (c) TRAIL^{-/-} mice with transplantation of WT BM. Indeed, mice that were transplanted with TRAIL-deficient BM displayed reduced alveolar AEC type I apoptosis (Fig. 9 A) and significantly reduced alveolar leakage on day 7 pi (Fig. 9 B) compared with mice that were transplanted

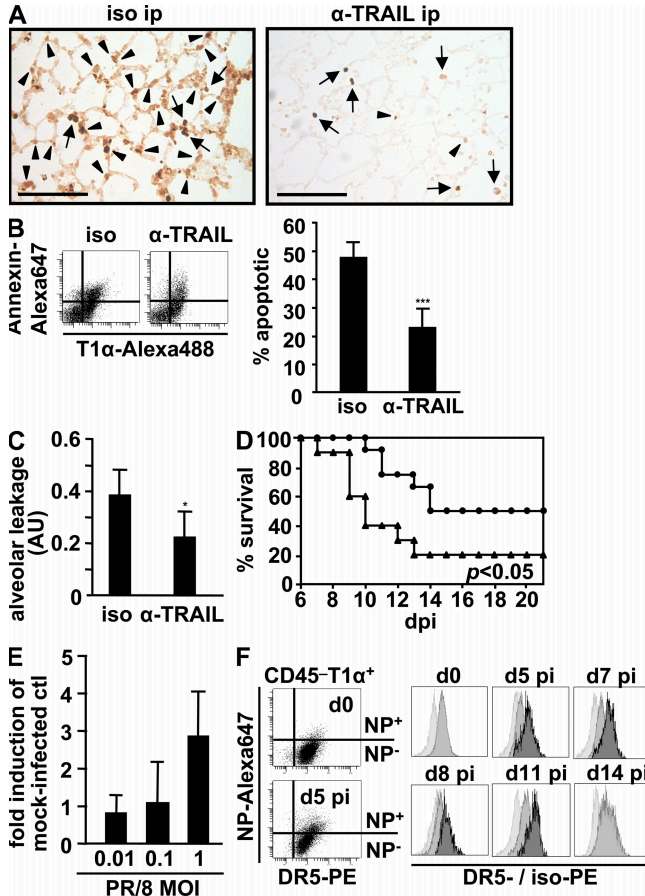


Figure 8. Anti-TRAIL treatment attenuates AEC apoptosis as well as alveolar leakage and enhances survival upon PR/8 infection. (A) PR/8-infected WT mice were treated with IgG isotype or anti-TRAIL mAb on days 3 and 5 pi and TUNEL assay was performed on lung cryosections at day 7 pi (arrows, apoptotic intraalveolar leukocytes; arrowheads, apoptotic AECs). Bars, 100 μ m. (B) FACS analysis (representative dot plots, left) and quantification (four to six mice per group; right) of apoptotic AEC I of PR/8-infected, IgG isotype-treated, or anti-TRAIL-treated mice (day 7 pi). Error bars show SD. (C) Alveolar leakage of PR/8-infected WT mice at day 7 pi that were treated with IgG isotype or anti-TRAIL mAb at days 3 and 5 pi. (D) Survival of PR/8-infected WT mice treated with isotype IgG (\blacktriangle , $n = 10$) or anti-TRAIL mAb (\bullet , $n = 12$) at days 3, 5, 7, and 9 pi in three independent experiments. (E) TRAIL receptor DR5 is expressed on cultured AEC and up-regulated upon PR/8 infection dose dependently in vitro. Bar graphs depict DR5 mRNA expression as fold induction of mock-infected AEC. (F) DR5 is expressed on AEC and up-regulated upon PR/8 infection in vivo. Left, FACS analysis of DR5 and NP expression of gated AEC type I (CD45⁻ T1 α ⁺) from digested lungs of uninfected (day 0, top) or PR/8-infected (day 5 pi) WT mice. Right, histograms depict DR5 expression of NP-negative (medium gray histograms) and NP-positive CD45⁻ T1 α ⁺ AEC I (dark gray histograms) from noninfected (day 0) and PR/8-infected WT mice in the time course of infection. Isotype PE-stained cells are shown in light gray histograms. An NP-positive population is missing at days 0 and 14 pi. Bar graphs in C and E represent the means \pm SD of three to five independent experiments. *, $P < 0.05$; ***, $P < 0.005$; iso, isotype IgG; NP, IV nucleoprotein.

with TRAIL^{+/+} BM, with mice of all transplantation groups recruiting comparable alveolar exudate macrophage numbers (not depicted). Inhibition of alveolar exudate macrophage recruitment by anti-CCR2 antibodies significantly reduced alveolar leakage in mice after transplantation of WT (TRAIL^{+/+})

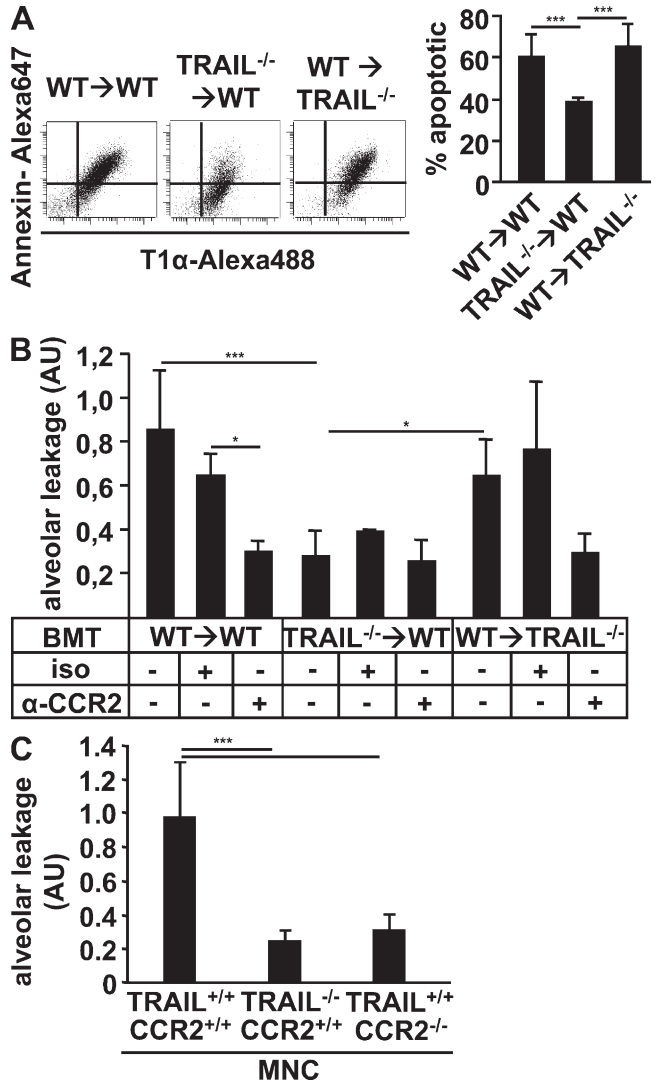


Figure 9. AEC apoptosis and lung leakage are reduced in PR/8-infected mice recruiting TRAIL-deficient exudate macrophages to their lungs. (A) Digested lungs of three different groups of PR/8-infected BM chimeric mice (WT recipient mice with transplantation of WT BM cells; WT recipient mice with transplantation of TRAIL^{-/-} BM cells; and TRAIL^{-/-} recipient mice with transplantation of WT BM cells) were analyzed for AEC type I apoptosis (left, representative FACS plots; right, quantitative analysis of five independent experiments). Error bars show SD. (B) Alveolar leakage of different BM chimeric mice that were either left untreated or injected with isotype IgG or anti-CCR2 mAb, respectively, was analyzed at day 7 pi. (C) CCR2^{-/-} mice were adoptively transferred with CCR2^{+/+}/TRAIL^{+/+}, CCR2^{+/+}/TRAIL^{-/-}, or CCR2^{-/-}/TRAIL^{+/+} MNC, and alveolar leakage was analyzed at day 7 after PR/8 infection. BMT, BM transplantation; iso, isotype IgG; MNC, mononuclear cells; ***, $P < 0.005$; *, $P < 0.05$. Bar graphs in B and C represent the means \pm SD of three to five mice per group from three independent experiments.

but not in mice after transplantation of TRAIL^{-/-} BM. These data indicate that TRAIL expression on grafted and then CCR2 dependently recruited cells rather than on lung resident cells is linked to lung injury. In addition, in an adoptive transfer approach using CCR2^{-/-} recipient mice that were either transferred TRAIL^{+/+}/CCR2^{+/+}, TRAIL^{-/-}/CCR2^{+/+}, or TRAIL^{+/+}/CCR2^{-/-} mononuclear cells, alveolar leakage was assessed upon PR/8 infection. In this model, CCR2-deficient recipient mice will largely recruit adoptively transferred CCR2^{+/+} monocytes into their lungs. As shown in Fig. 9 C, alveolar leakage at day 7 pi was significantly less in mice recruiting TRAIL-deficient compared with mice recruiting TRAIL^{+/+} exudate macrophages, with comparable alveolar exudate macrophage numbers in both treatment groups at day 7 pi (TRAIL^{+/+}/CCR2^{+/+} MNC, $5.79 \pm 1.02 \times 10^5$; TRAIL^{-/-}/CCR2^{+/+} MNC, $4.87 \pm 1.48 \times 10^5$). Recipient mice that were transferred CCR2^{-/-} MNC recruited only $1.62 \pm 0.99 \times 10^5$ exudate macrophages and correspondingly demonstrated low leakage. These data clearly demonstrate that TRAIL-induced lung injury in PR/8 pneumonia is mediated by alveolar recruitment of TRAIL^{+/+} but not TRAIL^{-/-} exudate macrophages.

DISCUSSION

IV pneumonia is characterized by the rapid development of acute lung injury with a poor outcome. One of the hallmarks of acute lung injury is an incremental alveolar barrier dysfunction followed by accumulation of protein-rich edema fluid in the alveolar compartment (12, 26, 27). Both viral pathogenicity factors and imbalanced host immune responses have been attributed a role in IV-induced lung failure (28–30). However, the molecular cross talk between immune and lung structural cell populations that leads to severe immunopathology and organ dysfunction is largely unknown.

Therefore, we tested the hypothesis that exudate macrophages, recruited to the lung in a CCL2/CCR2-dependent manner, might contribute to lung barrier dysfunction during lethal IV infection. In fact, alveolar barrier function, which is severely affected in IV-infected WT mice, was found to be significantly improved in CCR2-deficient mice exhibiting defective exudate macrophage recruitment. Consequently, CCR2 deficiency was associated with drastically decreased mortality during experimental IV pneumonia. Moreover, the pronounced lung leakage observed in WT mice correlated with an increased AEC apoptosis rate found to be induced by TRAIL, which is predominantly expressed in exudate lung macrophages. Finally, treatment of IV-infected WT mice with an anti-TRAIL mAb or use of mice recruiting TRAIL-deficient exudate macrophages not only attenuated alveolar leakage but significantly reduced mortality from IV pneumonia. Collectively, these results demonstrate that macrophage recruitment to IV-infected lungs in mice exerts detrimental effects on lung parenchymal cells of the highly sensitive gas exchange compartment severely affecting alveolar barrier function via TRAIL-induced epithelial apoptosis.

CCR2 is known to play a crucial role in host defense against pathogens. Interacting with its primary ligand CCL2

(MCP-1), CCR2 mediates the egress of GR1⁺ monocytes from the BM and their recruitment from peripheral blood to sites of infection (1, 23, 24, 31–33). In our own previous studies, we demonstrated that monocyte transmigration upon epithelial PR/8 infection in vitro was strictly dependent on the CCL2-CCR2 axis (4). Thus, we assumed that the reduced lung leakage and mortality observed in CCR2-deficient mice during IV infection might be attributed to abrogated pulmonary macrophage accumulation. In fact, as demonstrated by the use of chimeric mice, loss of alveolar barrier function was solely dependent on CCR2 expression on circulating monocytes, indicating that mononuclear phagocyte traffic was critically involved and that CCR2-positive resident lung cell populations did not contribute to increased lung permeability in our model. Interestingly, a reduction of lung macrophage recruitment by 50% resulted in an approximately fivefold decrease in alveolar leakage, suggesting that alveolar damage only occurs beyond a critical threshold of macrophage accumulation and that partial inhibition of macrophage recruitment during IV pneumonia may strongly attenuate lung injury while presumably maintaining critical macrophage host defense functions.

Several authors demonstrated both release of GR1⁺ monocytes from the BM into the circulation and their inflammatory organ recruitment to be CCR2 dependent, with CCR2^{-/-} mice exhibiting diminished peripheral blood monocyte counts (32, 33). Accordingly, GR1⁺ peripheral blood monocytes were revealed to be ~50% less in PR/8-infected CCR2-deficient mice and in anti-CCR2 mAb-treated mice in our study (unpublished data), confirming the aforementioned data and supporting the concept of CCR2 involvement in distinct steps of monocyte homeostasis under inflammatory and noninflammatory conditions. Additionally, direct antibody-mediated cytotoxicity might account for reduced GR1⁺ blood monocyte numbers in anti-CCR2 mAb-treated mice (34). Therefore, a contribution of reduced circulating monocyte numbers to the attenuation of acute lung injury in IV pneumonia cannot be totally excluded.

CCR2 deficiency was found to be associated with a slight but significant delay in viral clearance, confirming observations reported previously by Dawson et al. (1) who suggest delayed adaptive immune responses as the underlying mechanism. However, we were not able to detect significant differences in the alveolar accumulation of CD4⁺ or CD8⁺ T lymphocytes despite the observed delay in DC recruitment, which is known as the major APC population. Ongoing IV replication in CCR2^{-/-} mice seemingly had no effect on alveolar epithelial integrity. In fact, epithelial apoptosis occurred when exudate macrophages were alveolar recruited in PR/8-infected WT mice between days 7 and 14 pi. This correlated with the bulk of mortality that was observed when virus titers were already reduced ~100-fold and IV nucleoprotein detection in AECs declined. These data support the concept that macrophage-mediated immune pathology accounts for the severity of PR/8-induced lung injury in WT mice. Correspondingly, in a milder nonlethal model of IV

infection (x31) where exudate macrophage numbers were ~75% lower than in PR/8-infected WT mice, lung injury was considerably less pronounced, emphasizing the predominant role of host immune responses in IV-induced pathology.

Alveolar epithelial apoptosis has been described as a common feature of acute lung injury caused by direct or indirect factors such as pneumonia, aspiration, sepsis, or trauma (13–15). Apoptosis is a regulated form of cell death that is mediated by membrane death receptors (extrinsic pathway) and direct mitochondrial injury (intrinsic pathway). Apoptosis has been described to occur in the lungs of patients with acute lung injury by activation of the epithelial membrane Fas death receptor by soluble FasL, released from invading leukocytes and accumulating in a biologically active form at the onset of lung injury (35, 36). However, in our model of IV-induced acute lung injury, FasL transcripts were not differentially regulated in the macrophage subsets analyzed. In contrast, the proapoptotic molecule TRAIL not expressed in peripheral blood monocytes was found to be strongly up-regulated in exudate macrophages recruited into the alveolar space in IV-infected WT mice, whereas TRAIL was undetectable in the alveolar mononuclear phagocytes of IV-infected CCR2^{-/-} mice. TRAIL induction in alveolar exudate macrophages may be caused by the recruitment process into the lung itself or by inflammatory mediators present within the IV-infected alveolar compartment. Notably, TRAIL induction on recruited macrophages was observed in PR/8 infection, representing a very severe and highly inflammatory form of IV pneumonia in mice, but not in x31 infection, suggesting that TRAIL-mediated alveolar injury might be restricted to severe forms of IV pneumonia as observed during human H5N1 infections. Consistent with this, previous reports identified type I IFNs as potent inducers of TRAIL in monocytes and DCs (21, 37). Indeed, we found IFN- α to be alveolar released upon PR/8 infection in WT mice yet peaking early by day 2 pi (219 ± 78 pg/ml; unpublished data). TRAIL, acting as a membrane-bound or soluble form, has been known to induce apoptosis in various tumor cells but not in nonneoplastic cells (20, 21). Recently, TRAIL expressed on lymphocyte subpopulations, DCs, and monocyte-derived macrophages has been associated with antiviral host responses during IV infection (17, 18, 38), underlining the importance of death pathways in antiviral immunity. In contrast, Wurzer et al. (39) found TRAIL-induced programmed cell death pathways to be crucial for IV propagation in vitro. In mice, TRAIL exclusively acts via the membrane DR5 that is expressed on the target cell. Interestingly, DR5 was up-regulated in primary murine AECs in vitro and in vivo upon PR/8 infection, suggesting that a preceding epithelial IV infection might facilitate TRAIL-induced apoptosis as a potential host mechanism to limit viral spread. Indeed, in our model, PR/8 clearance revealed to be delayed in mice upon anti-TRAIL treatment. However, DR5 expression was also detectable in uninfected epithelial cells, indicating that exudate macrophage TRAIL may have the potential to attack noninfected epithelial cells as well when released in large amounts.

Consistent with this, the number of infected (NP⁺) AECs was only slightly reduced in WT compared with CCR2^{-/-} mice on days 11 and 14 pi, indicating only partial selectivity of TRAIL-mediated killing between infected and noninfected cells. These data suggest that, upon such conditions, the destructive effects of TRAIL prevail over its antiviral function thereby leading to enhanced lung injury and mortality.

A recent study (40) confirms the concept that monocyte-derived cells significantly contribute to immunopathology and lung injury in PR/8 pneumonia, but the authors suggest the underlying mechanism to be an increased production of inducible nitric oxide synthase and TNF- α . Regarding TNF- α release, we could not detect significant differences in alveolar-secreted TNF- α during the time course after PR/8 infection in WT and CCR2-deficient mice (unpublished data). As previously published by Akaike et al. (41), reactive oxygen and nitrogen species have been detected in the alveolar fluid of IV infected mice, and macrophages and neutrophils were identified as the primary source. Although Lin et al. (40) did not provide direct evidence that monocyte/macrophage-derived reactive nitrogen species accounted for the observed lung damage in their model, it is conceivable that macrophage-released proinflammatory mediators additionally contribute to lung injury in IV pneumonia.

Altogether, our study demonstrates for the first time a key role of exudate macrophage TRAIL in AEC apoptosis promoting alveolar barrier dysfunction during IV lung infection. Notably, inhibition of TRAIL activity largely protected mice from lethal IV pneumonia. Targeting the TRAIL-DR5 pathway might therefore be a suitable tool for restoring lung epithelial function in patients suffering from severe IV pneumonia.

MATERIALS AND METHODS

Reagents. The following anti-mouse mAbs/secondary reagents were used for flow cytometry: CD45.2-FITC and CD45.2-PerCP-Cy5.5 (30F-11), CD45.1-PE (A20), GR1-PE and GR1-FITC (RB6-8C5), GR1-PE-Cy7 (RB6-8C5), biotinylated I-A/I-E (2G9), NK1.1-APC (PK136), CD4-FITC (RM4-4), biotinylated CD8- α (53-6.7), CD11c-PE (HL3), CD11b-FITC (M1/70), SA-APC-Cy7, biotinylated F(ab')₂ anti-mouse Ig, Streptavidin-PE, isotype-matched control IgG antibodies (all BD), F4/80-Alexa Fluor 647 (CI:A3-1; Invitrogen), F4/80-Alexa Fluor 488 (BM8; Invitrogen), CD11c-PE-Cy5.5 (418; Invitrogen), CD115-PE (MCA1898; AbD Serotec), T1 α /Podoplanin/gp36 (Abcam), TRAIL-PE (N2B2; BioLegend), TRAIL R2 (DR5)-PE (118929; R&D Systems), isotype-PE (rat IgG2a κ ; BioLegend), antiinfluenza NP (Meridian Life Science, Inc.), annexin V-Alexa Fluor 647, anti-hamster Ig Alexa Fluor 488, and anti-mouse Ig Alexa Fluor 647 (all Invitrogen). 150 μ g of low endotoxin/azide-free anti-TRAIL mAb (N2B2; IgG2a; BioLegend) in 150 μ l PBS^{-/-} was applied i.p. at days 3, 5, 7, and 9 pi, and 75 μ g of rat anti-mouse CCR2 mAb (IgG2b; gift from M. Mack, University of Regensburg, Regensburg, Germany) in 100 μ l PBS^{-/-} was applied i.p. at days 0 and 4 pi (42). Respective isotype control IgG Abs (IgG2a [BioLegend] and IgG2b [BD]) were applied at the same concentrations. Propidium iodide was purchased from Sigma-Aldrich.

Mice. C57BL/6 WT mice were purchased from Charles River Laboratories. CCR2-deficient mice were generated as described previously and backcrossed to the C57BL/6 background (43). B6.SJL-*Ptpr^c* mice expressing the CD45.1 alloantigen (Ly5.1 PTP) on circulating leukocytes (C57BL/6 genetic background) were obtained from The Jackson Laboratory. TRAIL-deficient mice (C57BL/6 genetic background) were a gift from Amgen.

Mice were bred under specific pathogen-free conditions. All experiments were approved by the regional council (Regierungspräsidium) of Giessen.

Treatment protocols. Mice were intratracheally inoculated with 500 PFU of IV PR/8 (A/PR/8/34; H1N1) or with 50,000 PFU of A/HKx31 (x31; H3N2) diluted in sterile PBS^{-/-} in a total volume of 70 μ l or mock-infected with PBS^{-/-} alone, and blood and BAL leukocytes were gained and processed as previously outlined in detail (44). BAL cells were counted with a hemocytometer, and differential cell counts of Pappenheim-stained cytocentrifuge preparations were performed using overall morphological criteria, including differences in cell size and shape of nuclei. Alveolar leakage in treated mice was analyzed by the lung permeability assay by i.v. injection of FITC-labeled albumin as previously described (2). For apoptosis detection, perfused lungs from infected or mock-infected mice were digested as previously outlined in detail (4), washed, and resuspended in FACS buffer (PBS, 7.4% EDTA, and 0.5% FCS). For quantitative analysis of interstitial exudate macrophages, lavaged and perfused lung tissue from WT or CCR2-deficient mice was prepared as previously described (2) and resuspended in FACS buffer.

Lung virus titers. Lungs were mechanically homogenized in 2 ml PBS^{+/+} on ice and centrifuged at 4,000 rpm for 10 min at 4°C, and supernatants were serially diluted (1:10⁰ to 1:10⁷) in PBS/BA containing 0.2% BSA, 1 mM MgCl₂, 0.9 mM CaCl₂, 100 U/ml of penicillin, and 0.1 mg/ml of streptomycin. Virus titers were determined by immunohistochemistry on confluent Madin-Darby canine kidney cells in 96-well plates in duplicates. In brief, cells were incubated with 50 μ l of homogenate dilution for 1 h at room temperature and covered with 1.5% methylcellulose media containing 2 μ g/ml trypsin (PAA) for 72 h. Cells were permeabilized and fixed with PBS^{+/+}/4% PFA/1% Triton X-100, incubated with diluted primary anti-PR/8 nucleoprotein mAb (Biozol) and secondary HRP-conjugated anti-mouse antibody for 45 min each, and stained with an AEC staining kit (Sigma-Aldrich) for 10 min. Foci were counted using a light microscope (DM 2500; Leica).

Flow cytometry and cell sorting. 1–5 \times 10⁵ PFA-fixed cells were washed in either FACS or annexin V staining buffer (10 mM Hepes, 140 mM NaCl, and 2.5 mM CaCl₂), incubated with the respective primary and secondary mAbs, and flow cytometric analysis was performed using a FACSCanto flow cytometer (BD) as previously described (2). Cells stained with primary CCR2 mAb were coupled with biotinylated F(ab')₂ anti-Ig for 30 min before a 15-min incubation with Streptavidin-PE. For cell sorting experiments, unfixed blood or BAL cells from eight mice per experiment were incubated with the given mAbs and high purity sorted with a FACS Vantage SE flow cytometer as previously outlined in detail (2). Purities of sorted cell population were always >90%.

ELISA. Cytokine levels from BALF were analyzed using commercially available ELISA kits (R&D Systems) according to the manufacturer's instructions. Detection limits were 2 pg/ml for CCL2, 5.1 pg/ml for TNF- α , and 12.5 pg/ml for IFN- α .

Creation of BM chimeric mice. BM cells were isolated under sterile conditions from the tibias and femurs of WT C57BL/6 or from CCR2^{-/-} or TRAIL^{-/-} donor mice as described previously (25). In some experiments, WT and CCR2^{-/-} BM cells were mixed at a 1:1 ratio before transplantation. As controls for BM engraftment, WT C57BL/6 BM cells (expressing the CD45.2 alloantigen) were transplanted into CD45.1 alloantigen-expressing C57BL/6 mice ($n = 2$ during each transplantation experiment), and the proportion of CD45.2-positive peripheral blood leukocytes was analyzed by flow cytometry. BM engraftment was 90.5 \pm 2.7% 2 wk after transplantation. Chimeric mice were housed under specific pathogen-free conditions for 14 d before PR/8 infection.

Preparation of lung tissue sections and TUNEL assay. Perfused lungs were carefully lavaged with 400- μ l aliquots of PBS^{-/-}/2 mM EDTA to

wash out alveolar leukocytes and were thereafter slowly inflated with 1.5 ml of a 1:1 mixture of Tissue-Tek OCT (Sakura) and PBS^{-/-}, removed en bloc, and snap frozen in liquid nitrogen. Lung tissue cryosections were mounted on glass slides and dried overnight at room temperature. Apoptotic cells were stained using the DeadEnd Colorimetric TUNEL system (Promega) according to the manufacturer's instructions. Slides were analyzed with a light microscope (DM 2000; Leica) at the indicated magnification using digital imaging software (Leica).

RNA isolation and real time RT-PCR. RNA from sorted blood or BAL cells was isolated using the RNeasy Micro kit (QIAGEN), whereas RNA from cultured AECs was isolated by PeqGOLD Total RNA kit (PEQLAB) according to the manufacturer's instructions. For cDNA synthesis, reagents and incubation steps were performed as described previously (2). Reactions were performed in an ABI 7900 Sequence Detection System (Applied Biosystem) using SYBR-Green I as fluorogenic probe in 25- μ l reactions containing 5 μ l cDNA sample, Platinum SYBR Green qPCR Super-Mix (Invitrogen), and 45 pmol of forward and reverse primers. The following primer sequences were used: TNF- α forward, 5'-CATCTTCTCAA-AATTCGAGTGACAA-3', and reverse, 5'-TGGGAGTAGACAAGG-TACAACCC-3'; FasL forward, 5'-CCAACCAAGCCTTAAAGTAT-CATC-3', and reverse, 5'-AACCCAGTTTCGTTGATCACA-3'; TRAIL forward, 5'-GAAGACCTCAGAAAGTGGC-3', and reverse, 5'-GAC-CAGCTCTCCATTCCTA-3'; DR5 forward, 5'-AAGTGTGTCTC-CAAAACGG-3', and reverse, 5'-AATGCACAGAGTTCGCACT-3'; and PBGD forward, 5'-GGTACAAGGCTTTCAGCATCG-3', and reverse, 5'-ATGTCCGGTAACGGCGGC-3'. Relative expression was determined by the 2 ^{$\Delta\Delta$ CT} method.

AEC isolation and infection. AECs were isolated from untreated WT mice, cultured for 5 d, and infected with influenza A virus at the indicated multiplicity of infection for 8 h as previously described in detail (4).

Adoptive transfer of PBMC. For isolation of PBMCs, whole blood cells gained from WT, TRAIL^{-/-}, or CCR2^{-/-} mice were carefully layered over 3 ml Lympholyte (Biozol). Cells were centrifuged at 1,400 rpm at room temperature for 35 min to separate the mononuclear fraction. The interphase was collected and mononuclear cells were washed twice in RPMI 1640. 2 \times 10⁶ MNC in 150 μ l RPMI were injected i.v. directly before PR/8 infection into CCR2^{-/-} mice. Purity of MNC was always >90%, as assessed by differential counts on Pappenheim-stained cytocentrifuge preparations.

Statistical analysis. All data are given as the mean \pm SD. For analysis of statistical differences, one-factor ANOVA was applied. Statistical significances between treatment groups were calculated with the SPSS for Windows software program (SPSS, Inc.). Significance was assumed when P values were <0.05.

Online supplemental material. Fig. S1 shows the time course of interstitial lung exudate macrophage proportions in PR/8-infected WT and CCR2-deficient mice. Fig. S2 shows the time course of viral titers in lung homogenate of PR/8-infected untreated or anti-TRAIL-treated WT mice. Online supplemental material is available at <http://www.jem.org/cgi/content/full/jem.20080201/DC1>.

The authors wish to thank P. Janssen, M. Lohmeyer, E. Braun, and D. Hensel for excellent technical assistance.

This work was supported by the German Research Foundation, grant SFB 547 "Cardiopulmonary Vascular System," the Excellence Cluster Cardio-Pulmonary System (ECCPS), the National Network on Community-Acquired Pneumonia (CAPNETZ), and the Clinical Research Group "Infectious Diseases" 01 KI 0770.

The authors have no conflicting financial interests.

Submitted: 30 January 2008

Accepted: 12 November 2008

REFERENCES

- Dawson, T.C., M.A. Beck, W.A. Kuziel, F. Henderson, and N. Maeda. 2000. Contrasting effects of CCR5 and CCR2 deficiency in the pulmonary inflammatory response to influenza A virus. *Am. J. Pathol.* 156:1951–1959.
- von Wulffen, W., M. Steinmueller, S. Herold, L.M. Marsh, P. Bulau, W. Seeger, T. Welte, J. Lohmeyer, and U.A. Maus. 2007. Lung dendritic cells elicited by Fms-like tyrosine 3-kinase ligand amplify the inflammatory response to lipopolysaccharide. *Am. J. Respir. Crit. Care Med.* 176:892–901.
- Fogg, D.K., C. Sibon, C. Miled, S. Jung, P. Aucouturier, D.R. Littman, A. Cumano, and F. Geissmann. 2006. A clonogenic bone marrow progenitor specific for macrophages and dendritic cells. *Science*. 311:83–87.
- Herold, S., W. von Wulffen, M. Steinmueller, S. Pleschka, W.A. Kuziel, M. Mack, M. Srivastava, W. Seeger, U.A. Maus, and J. Lohmeyer. 2006. Alveolar epithelial cells direct monocyte transepithelial migration upon influenza virus infection: impact of chemokines and adhesion molecules. *J. Immunol.* 177:1817–1824.
- Maus, U., K. von Grote, W.A. Kuziel, M. Mack, E.J. Miller, J. Cihak, M. Stangassinger, R. Maus, D. Schlondorff, W. Seeger, and J. Lohmeyer. 2002. The role of CC chemokine receptor 2 in alveolar monocyte and neutrophil immigration in intact mice. *Am. J. Respir. Crit. Care Med.* 166:268–273.
- Tacke, F., and G.J. Randolph. 2006. Migratory fate and differentiation of blood monocyte subsets. *Immunobiology*. 211:609–618.
- Taut, K., C. Winter, D.E. Briles, J.C. Paton, J.W. Christman, R. Maus, R. Baumann, T. Welte, and U.A. Maus. 2007. Macrophage turnover kinetics in the lungs of mice infected with *Streptococcus pneumoniae*. *Am. J. Respir. Cell Mol. Biol.* 38:105–113.
- Cheung, C.Y., L.L. Poon, A.S. Lau, W. Luk, Y.L. Lau, K.F. Shorridge, S. Gordon, Y. Guan, and J.S. Peiris. 2002. Induction of proinflammatory cytokines in human macrophages by influenza A (H5N1) viruses: a mechanism for the unusual severity of human disease? *Lancet*. 360:1831–1837.
- Lee, D.C., C.Y. Cheung, A.H. Law, C.K. Mok, M. Peiris, and A.S. Lau. 2005. p38 mitogen-activated protein kinase-dependent hyperinduction of tumor necrosis factor alpha expression in response to avian influenza virus H5N1. *J. Virol.* 79:10147–10154.
- Kash, J.C., T.M. Tumpey, S.C. Prohl, V. Carter, O. Perwitasari, M.J. Thomas, C.F. Basler, P. Palese, J.K. Taubenberger, A. Garcia-Sastre, et al. 2006. Genomic analysis of increased host immune and cell death responses induced by 1918 influenza virus. *Nature*. 443:578–581.
- Tran, T.H., T.L. Nguyen, T.D. Nguyen, T.S. Luong, P.M. Pham, V.C. Nguyen, T.S. Pham, C.D. Vo, T.Q. Le, T.T. Ngo, B.K. Dao, P.P. Le, T.T. Nguyen, T.L. Hoang, V.T. Cao, T.G. Le, D.T. Nguyen, H.N. Le, K.T. Nguyen, H.S. Le, V.T. Le, D. Christiane, T.T. Tran, M. de Jong, C. Schultz, P. Cheng, W. Lim, P. Horby, and J. Farrar. 2004. Avian influenza A (H5N1) in 10 patients in Vietnam. *N. Engl. J. Med.* 350:1179–1188.
- Arabi, Y., C.D. Gomersall, Q.A. Ahmed, B.R. Boynton, and Z.A. Memish. 2007. The critically ill avian influenza A (H5N1) patient. *Crit. Care Med.* 35:1397–1403.
- Perl, M., C.S. Chung, U. Perl, J. Lomas-Neira, M. de Paep, W.G. Cioffi, and A. Ayala. 2007. Fas-induced pulmonary apoptosis and inflammation during indirect acute lung injury. *Am. J. Respir. Crit. Care Med.* 176:591–601.
- Kitamura, Y., S. Hashimoto, N. Mizuta, A. Kobayashi, K. Kooguchi, I. Fujiwara, and H. Nakajima. 2001. Fas/FasL-dependent apoptosis of alveolar cells after lipopolysaccharide-induced lung injury in mice. *Am. J. Respir. Crit. Care Med.* 163:762–769.
- Guinee, D. Jr., E. Brambilla, M. Fleming, T. Hayashi, M. Rahn, M. Koss, V. Ferrans, and W. Travis. 1997. The potential role of BAX and BCL-2 expression in diffuse alveolar damage. *Am. J. Pathol.* 151:999–1007.
- Benedict, C.A., T.A. Banks, and C.F. Ware. 2003. Death and survival: viral regulation of TNF signaling pathways. *Curr. Opin. Immunol.* 15:59–65.
- Zhou, J., H.K. Law, C.Y. Cheung, I.H. Ng, J.S. Peiris, and Y.L. Lau. 2006. Functional tumor necrosis factor-related apoptosis-inducing ligand production by avian influenza virus-infected macrophages. *J. Infect. Dis.* 193:945–953.
- Ishikawa, E., M. Nakazawa, M. Yoshinari, and M. Minami. 2005. Role of tumor necrosis factor-related apoptosis-inducing ligand in immune response to influenza virus infection in mice. *J. Virol.* 79:7658–7663.
- Finnberg, N., J.J. Gruber, P. Fei, D. Rudolph, A. Bric, S.H. Kim, T.F. Burns, H. Ajuha, R. Page, G.S. Wu, et al. 2005. DR5 knockout mice are compromised in radiation-induced apoptosis. *Mol. Cell. Biol.* 25:2000–2013.
- Cretney, E., K. Takeda, H. Yagita, M. Glaccum, J.J. Peschon, and M.J. Smyth. 2002. Increased susceptibility to tumor initiation and metastasis in TNF-related apoptosis-inducing ligand-deficient mice. *J. Immunol.* 168:1356–1361.
- Griffith, T.S., S.R. Wiley, M.Z. Kubin, L.M. Sedger, C.R. Maliszewski, and N.A. Fanger. 1999. Monocyte-mediated tumoricidal activity via the tumor necrosis factor-related cytokine, TRAIL. *J. Exp. Med.* 189:1343–1354.
- Peters, W., J.G. Cyster, M. Mack, D. Schlondorff, A.J. Wolf, J.D. Ernst, and I.F. Charo. 2004. CCR2-dependent trafficking of F4/80dim macrophages and CD11c dim/intermediate dendritic cells is crucial for T cell recruitment to lungs infected with *Mycobacterium tuberculosis*. *J. Immunol.* 172:7647–7653.
- Winter, C., K. Taut, M. Srivastava, F. Langer, M. Mack, D.E. Briles, J.C. Paton, R. Maus, T. Welte, M.D. Gunn, and U.A. Maus. 2007. Lung-specific overexpression of CC chemokine ligand (CCL) 2 enhances the host defense to *Streptococcus pneumoniae* infection in mice: role of the CCL2-CCR2 axis. *J. Immunol.* 178:5828–5838.
- Robben, P.M., M. LaRegina, W.A. Kuziel, and L.D. Sibley. 2005. Recruitment of Gr-1⁺ monocytes is essential for control of acute toxoplasmosis. *J. Exp. Med.* 201:1761–1769.
- Maus, U.A., K. Waelisch, W.A. Kuziel, T. Delbeck, M. Mack, T.S. Blackwell, J.W. Christman, D. Schlondorff, W. Seeger, and J. Lohmeyer. 2003. Monocytes are potent facilitators of alveolar neutrophil emigration during lung inflammation: role of the CCL2-CCR2 axis. *J. Immunol.* 170:3273–3278.
- Xu, T., J. Qiao, L. Zhao, G. Wang, G. He, K. Li, Y. Tian, M. Gao, J. Wang, H. Wang, and C. Dong. 2006. Acute respiratory distress syndrome induced by avian influenza A (H5N1) virus in mice. *Am. J. Respir. Crit. Care Med.* 174:1011–1017.
- Morty, R.E., O. Eickelberg, and W. Seeger. 2007. Alveolar fluid clearance in acute lung injury: what have we learned from animal models and clinical studies? *Intensive Care Med.* 33:1229–1240.
- Tumpey, T.M., C.F. Basler, P.V. Aguilar, H. Zeng, A. Solorzano, D.E. Swayne, N.J. Cox, J.M. Katz, J.K. Taubenberger, P. Palese, and A. Garcia-Sastre. 2005. Characterization of the reconstructed 1918 Spanish influenza pandemic virus. *Science*. 310:77–80.
- Tumpey, T.M., A. Garcia-Sastre, J.K. Taubenberger, P. Palese, D.E. Swayne, M.J. Pantin-Jackwood, S. Schultz-Cherry, A. Solorzano, N. Van Rooijen, J.M. Katz, and C.F. Basler. 2005. Pathogenicity of influenza viruses with genes from the 1918 pandemic virus: functional roles of alveolar macrophages and neutrophils in limiting virus replication and mortality in mice. *J. Virol.* 79:14933–14944.
- Szretter, K.J., S. Gangappa, X. Lu, C. Smith, W.J. Shieh, S.R. Zaki, S. Sambhara, T.M. Tumpey, and J.M. Katz. 2007. Role of host cytokine responses in the pathogenesis of avian H5N1 influenza viruses in mice. *J. Virol.* 81:2736–2744.
- Hokeness, K.L., W.A. Kuziel, C.A. Biron, and T.P. Salazar-Mather. 2005. Monocyte chemoattractant protein-1 and CCR2 interactions are required for IFN-alpha/beta-induced inflammatory responses and antiviral defense in liver. *J. Immunol.* 174:1549–1556.
- Tsou, C.L., W. Peters, Y. Si, S. Slaymaker, A.M. Aslanian, S.P. Weisberg, M. Mack, and I.F. Charo. 2007. Critical roles for CCR2 and MCP-3 in monocyte mobilization from bone marrow and recruitment to inflammatory sites. *J. Clin. Invest.* 117:902–909.
- Serbina, N.V., and E.G. Pamer. 2006. Monocyte emigration from bone marrow during bacterial infection requires signals mediated by chemokine receptor CCR2. *Nat. Immunol.* 7:311–317.
- Bruhl, H., J. Cihak, J. Plachy, L. Kunz-Schughart, M. Niedermeier, A. Denzel, M. Rodriguez Gomez, Y. Talke, B. Luckow, M. Stangassinger, and M. Mack. 2007. Targeting of Gr-1⁺, CCR2⁺ monocytes in collagen-induced arthritis. *Arthritis Rheum.* 56:2975–2985.

35. Martin, T.R., M. Nakamura, and G. Matute-Bello. 2003. The role of apoptosis in acute lung injury. *Crit. Care Med.* 31:S184–S188.
36. Martin, T.R., N. Hagimoto, M. Nakamura, and G. Matute-Bello. 2005. Apoptosis and epithelial injury in the lungs. *Proc. Am. Thorac. Soc.* 2:214–220.
37. Liu, S., Y. Yu, M. Zhang, W. Wang, and X. Cao. 2001. The involvement of TNF-alpha-related apoptosis-inducing ligand in the enhanced cytotoxicity of IFN-beta-stimulated human dendritic cells to tumor cells. *J. Immunol.* 166:5407–5415.
38. Chaperot, L., A. Blum, O. Manches, G. Lui, J. Angel, J.P. Molens, and J. Plumas. 2006. Virus or TLR agonists induce TRAIL-mediated cytotoxic activity of plasmacytoid dendritic cells. *J. Immunol.* 176:248–255.
39. Wurzer, W.J., C. Ehrhardt, S. Pleschka, F. Berberich-Siebelt, T. Wolff, H. Walczak, O. Planz, and S. Ludwig. 2004. NF-kappaB-dependent induction of tumor necrosis factor-related apoptosis-inducing ligand (TRAIL) and Fas/FasL is crucial for efficient influenza virus propagation. *J. Biol. Chem.* 279:30931–30937.
40. Lin, K.L., Y. Suzuki, H. Nakano, E. Ramsburg, and M.D. Gunn. 2008. CCR2+ monocyte-derived dendritic cells and exudate macrophages produce influenza-induced pulmonary immune pathology and mortality. *J. Immunol.* 180:2562–2572.
41. Akaike, T., Y. Noguchi, S. Ijiri, K. Setoguchi, M. Suga, Y.M. Zheng, B. Dietzschold, and H. Maeda. 1996. Pathogenesis of influenza virus-induced pneumonia: involvement of both nitric oxide and oxygen radicals. *Proc. Natl. Acad. Sci. USA.* 93:2448–2453.
42. Mack, M., J. Cihak, C. Simonis, B. Luckow, A.E. Proudfoot, J. Plachy, H. Bruhl, M. Frink, H.J. Anders, V. Vielhauer, et al. 2001. Expression and characterization of the chemokine receptors CCR2 and CCR5 in mice. *J. Immunol.* 166:4697–4704.
43. Kuziel, W.A., S.J. Morgan, T.C. Dawson, S. Griffin, O. Smithies, K. Ley, and N. Maeda. 1997. Severe reduction in leukocyte adhesion and monocyte extravasation in mice deficient in CC chemokine receptor 2. *Proc. Natl. Acad. Sci. USA.* 94:12053–12058.
44. Maus, U., S. Herold, H. Muth, R. Maus, L. Ermert, M. Ermert, N. Weissmann, S. Rosseau, W. Seeger, F. Grimminger, and J. Lohmeyer. 2001. Monocytes recruited into the alveolar air space of mice show a monocytic phenotype but upregulate CD14. *Am. J. Physiol. Lung Cell. Mol. Physiol.* 280:L58–L68.